Experimentation and theory leading to the understanding of biphoton interference

A. C. Bernstein

Department of Physics and Astronomy, University of New Mexico, Albuquerque, New Mexico, 87131

(Received 9 December 1999)

The use of spontaneous parametric down-conversion (SPDC) to produce the entangled two-photon state (called the biphoton state) for experimental purposes is relatively new. This paper explores the early experimentation and theoretical treatment of Hong, Ou, and Mandel (HOM) upon their entangled photon interferometer. The photon-photon interference picture of this experiment is compared with an HOM interferometer which is slightly modified. The modified HOM interferometer demonstrates the necessity for considering all possible path amplitudes of a self-interfering biphoton and shows the limitations of the photon-photon interference picture. These theoretical and experimental studies foster a deeper practical understanding of quantum coherence and provide examples of uniquely quantum behavior.

PACS numbers: 42.50.Ar, 03.65.Bz, 07.60.Ly, 2.20.Fv

I. INTRODUCTION

Despite the demonstration of the theoretical rigor of quantum optics in explaining experimental results [1], it is humbling to realize that optical interference experiments are still being carried out – indicating a still developmental stage of quantum optics and the physical understanding of results. A system commonly studied is the biphoton whereby two photons are generated by the same quantum event and are hence entangled. The description of these experiments can hardly be complete without a theoretical and experimental overview of photon-pair production processes [2,3], and the detection process [4]. These are subjects in and of themselves which in turn introduce concepts such as the EPR paradox [5], complementarity [6], and quantum entanglement [7]. Hence, this paper is not a historical review of the field, but rather of theoretical and experimental elements, cogent to the clear understanding of the system quantum state and its interference and coherence properties.

The standard way of producing an entangled two-photon state is through spontaneous parametric down-conversion (SPDC). Typically, a UV beam interacts with a nonlinear medium. The nonlinear interaction acts to "split" the incident photon into two output photons, the signal and idler, of lower frequencies, ω_1 and ω_2, where $\omega_p = \omega_1 + \omega_2$. In this photon-pair production process only ω_p is well defined whereas ω_1 and ω_2 can vary, but must satisfy the energy conserving frequency-sum condition

above. In practice, sets of apertures and interference filters select degenerate photon pairs ($\omega_1 \cong \omega_2$) which result from the crystal phase-matched condition, $\vec{k}_p = \vec{k}_i + \vec{k}_s$. The actual bandwidth of this selection determines the bandwidth of the detected photon wave-packets. See [8] for a review of relevant coherence properties of the SPDC process.

The *j*th beam with a conically spread wave-number, **k,** at the output of the nonlinear medium is quantized with the electric field operator [3]

$$\hat{E}_j^{(+)}(t) = \sum_k E_{jk} \hat{a}_{jk} e^{i(\mathbf{k}\cdot\mathbf{r} - \omega_{jk} t)} \tag{1}$$

where

$$E_{jk} = i\left[\frac{\hbar\omega_{jk}}{2\varepsilon_0 n_{jk} V_Q}\right]^{1/2}; \tag{2}$$

n_{jk} is the index of refraction experienced by the *j*th photon at frequency ω_{jk}; V_Q is the quantization volume. The pump field is a classical wave-packet with relatively long coherence time modeled as,

$$E_p^{(+)}(t) = E_0 e^{-t^2/\tau_p^2} e^{i(k_p z - \omega_p t)}. \tag{3}$$

To the first order in perturbation theory the signal-idler pair is (ignoring the vacuum component)

$$|\Psi\rangle = \int d\omega_p \, F(\omega_p) \, d^3\vec{k} \, d^3\vec{k}' \, \delta(\omega_p - \omega_s(\vec{k}) - \omega_i(\vec{k}')) \, \delta(\vec{k}_p' - \vec{k} - \vec{k}') \, a_s(\vec{k}) \, a_i(\vec{k}') |0\rangle \tag{4}$$

where all the constants and slowly varying functions have been taken under $F(\omega_p)$ which varies as a Gaussian. The delta function in *k*-space indicates the phase matched condition which the apertures are carefully arranged to fulfill. The limits of the integration are defined by interference filters placed before the detection equipment. Additional terms in the expansion are not necessary because the probability amplitudes for the generation of further photon-pairs are much smaller. Again, the degree to which $\omega_s(\vec{k}) = \omega_i(\vec{k}')$ is determined by interference filters placed before the detectors. So we may write

$$|\Psi\rangle = \int d\omega \, F(\omega) \left| \omega_s, \omega_i = \omega_p - \omega_s \right\rangle \tag{5}$$

where $F(\omega)$ is now a weighting function peaked at $\omega = \omega_p / 2 = \omega_i = \omega_s$ [9].

II. THE HONG, OU, MANDEL, EXPERIMENT AND MUTUAL PHOTON INTERFERENCE

To demonstrate the salient features of biphoton interference we examine two experiments. The first is an early biphoton interference experiment, the title of which belies a main motivation of resolving short optical pulse information, not introducing an entire class of quantum optical experiments: "Measurement of Subpicosecond Time Intervals between Two Photons by Interference," performed by Hong, Ou, and Mandel (HOM) [9]. In this experiment, two photons are generated by SPDC. Here, an Argon-ion beam of frequency ω_p (corresponding to the 351.1 nm line) interacts with an 8 cm long nonlinear crystal of potassium dihydrogen phosphate (KDP). The apertured interference filters have a bandwidth of 5×10^{12} Hz ($\omega_1 \cong \omega_2$) which result from the mode-matched condition. Figure 1 shows the setup. The coincidence rate of D1 and D2 is determined by counting detections occurring within the 7 ns temporal resolution of the counter. Hence, ignoring incidentals, only if both photons reflect (rr case) or both transmit (tt case) through the beam splitter will coincidences occur. The beam splitter can be adjusted an amount $\delta x = \delta\tau \cdot c$, say, to vary the pathlength associated with each possibility. This slowly introduces distinction between the different paths which affects the coincidence count. The coincident counting is the 4th order interference of the field, or intensity correlation [4],

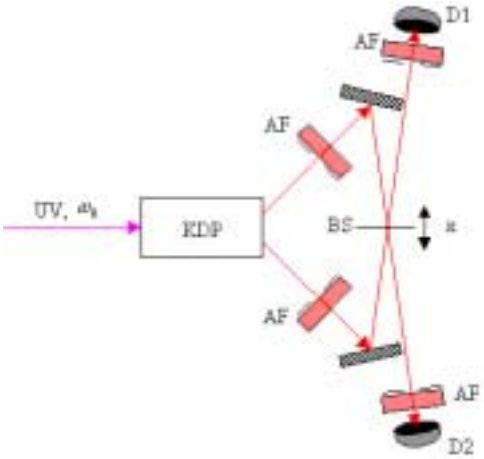

Fig. 1. Diagram of the Hou, Ou, Mandel optical setup. AF denotes the Aperture-interference filter combinations. The BS is the beam-splitter, and D1 and D2 are photomultiplier detectors.

$$P_{12}(\tau) = K\left\langle \hat{E}_1^{(-)}(t)\hat{E}_2^{(-)}(t+\tau)\hat{E}_2^{(+)}(t+\tau)\hat{E}_1^{(+)}(t)\right\rangle \qquad (6)$$

Where, for example, $\hat{E}_2^{(+)}(t+\tau)$ is the positive frequency component of the field operator at D2 which caused the detector to fire at a time difference of τ *after* D1 (for *positive* τ); K is a constant scaling the detector efficiency. For any single position of the beam-splitter τ varies as a Gaussian. It should be noted here that the photon beam temporal coherence is not longer than the several nanosecond resolution of the counter. Hence, the sinusoidal second order interference that would be present with a variation of $\delta\tau$ is not present at either detector. If we assume ideal degenerate mode-matching with $\delta\tau = 0$ to obtain probability amplitudes for the tt and rr cases, we obtain

$$\hat{E}_1^{(+)}(t) = \sqrt{T}\hat{E}_i^{(+)}(t) + i\sqrt{R}\hat{E}_s^{(+)}(t) \qquad \hat{E}_2^{(+)}(t) = \sqrt{T}\hat{E}_s^{(+)}(t) + i\sqrt{R}\hat{E}_i^{(+)}(t) \qquad (7)$$

$$\hat{E}_{1,2}^{(-)}(t) = \left[\hat{E}_{1,2}^{(+)}(t)\right]^{\dagger} .$$

Putting (7) into (6) results in,

$$P_{12}(\tau) = K\left(T^2 + R^2 - 2RT\right) = 0\,, \tag{8}$$

for a 50/50 beam-splitter. So there are no coincidence counts for this ideal condition. In reality, the finite bandwidth of ω_i and ω_s is demonstrated as the beam-splitter is moved from this null position, making a nominally non-stochastic delay of $2\delta\tau$ between detection times. Over the integration time, the finite bandwidth leads to,

$$N_c = C\left[T^2 + R^2 - 2RT\,\frac{\int_{-\infty}^{\infty} g(\tau)g(\tau - 2\delta\tau)d\tau}{\int_{-\infty}^{\infty} g^2(\tau)d\tau}\right], \tag{9}$$

where $g(\tau)$ is the normalized Fourier transform of $F(\omega)$ and represents the temporal width associated with the interference filters. Multiplying the last term in Eq. (9) is a normalized temporal convolution of the two photons wavepackets. The integration limits are infinite because this temporal width is much greater than the coherence time of the photons. For a Gaussian $F(\omega)$ we let

$$g(\tau) = e^{-(\Delta\omega\,\delta\tau)^2/2} \tag{10}$$

so that (9) becomes

$$N_c = C(T^2 + R^2)\left[1 - \frac{2RT}{R^2 + T^2}e^{-(\Delta\omega\,\delta\tau)^2}\right]. \tag{11}$$

The results of this equation and experimental data are shown in Fig. 2. The solid line is calculated using Eq. (11) for the experimentally derived value of $R/T = 0.95$. Incomplete contrast in the data is most likely due to imperfectly aligned beams, introducing a slight distinguishability in the two paths. The 16-μm bandwidth of the coincidence dip corresponds to 100 fs of relative delay, corresponding to the temporal coherence defined by the interference filter passband. The visibility of this dip is about 100%, twice that expected for classical field amplitudes [10].

This experiment, then, resolves the temporal coherence of the photon wave-packets. These strictly quantum effects are visible because the biphoton is a quantum phenomenon as represented in theory by the state-vector describing all possible paths. Detection schemes nonlinear in the field, such as the Hanbury-Brown—Twiss arrangement as used in this case, brings out the quantum nature of the biphoton. The authors' analysis was that the interference was simply between the individual photon E-field amplitudes,

and that the dip-width was a measure of the temporal convolution of the two single-photon wave packets. By describing the coincident E-field at the detectors then, the indistinguishable pathways were automatically summed and squared. This is a very classical concept which works because the photons are incident on the beam-splitter at the same time. The next experiment introduces a more generally correct way to think of the signal and idler photons, and the *single* quantum state they describe.

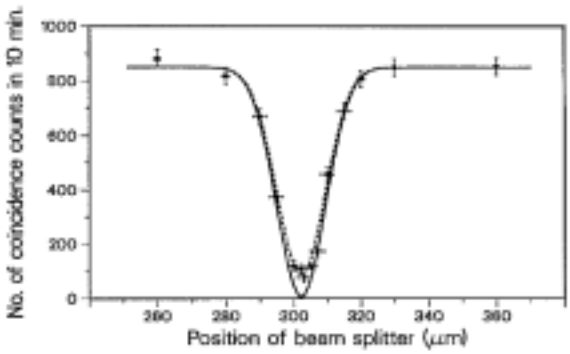

Fig. 2 The experimental near 100% interference dip in coincidence counts (dashed curve). Solid curves represent the theoretical and fitted theoretical results expected from Eq. (11) (after Hong *et al.*, 1987) [9].

II. THE STREKALOV, PITTMAN, SHIH EXPERIMENT AND THE BIPHOTON SELF-INTERFERENCE

Ideas in quantum optics commonly evolve through gedanken experiments specifically devised to demonstrate differences between classical and quantum-mechanical concepts. A model example of this approach can be studied in [11]. Similarly, after the HOM experiments, another generation of experiments emerged, specifically to demonstrate that the interference observed in the HOM experiment was not due to any local mutual interaction of the photons at the beam splitter (a classical phenomenon), but really the interference of the different possible path amplitudes of the single biphoton state. That is, the biphoton interferes with itself. Typically, the experiments keep the two photon incidences at the beam-splitter spacelike so that they never coincide at the beam-splitter at the same time (e.g., [12], [13], [14]). Most experiments have the quantum mechanical expectation of 100% interference visibility, but result in less-than 50% [14]. This leaves open the possibility of a classical, hidden-variable, interpretation of results. Recently a spacelike experiment by Strekalov, Pittman, and Shih (SPS) [13], succeeded in eliminating the hidden-variable interpretation by producing a nearly 100% visibility result.

In its construction, the SPS interferometer is merely a variation of the HOM interferometer, but its interpretation forces a more complete analysis of the biphoton. In this experiment, as shown in Fig. 3,

$L_S < L_0 < L_L$ such that, for $\delta x = 0$, $L_L - L_0 = L_0 - L_S = \Delta L$. In this way, upon emerging from the KDP, each photon can travel three possible distances. ΔL is within the dynamic range of the BS adjustability when $2\delta x = \Delta L = 2c\delta\tau$. It seems clear that there should be two coincidence dips for $\pm 2\delta x = \Delta L$, the delay-compensation positions of the beam-splitter. Because only half the photons have either path length L_S or L_L, then over the integration time of the detection, these dips should now have 50% visibility. Taking the approach of HOM, then, it also seems clear that no interference will occur

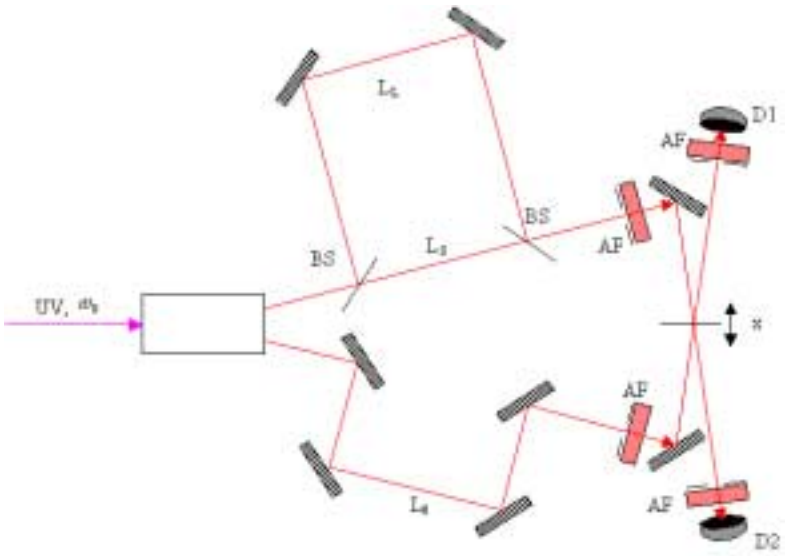

Fig. 3. Scheme of the SPS experiment. L_S and L_L are the short and long pathlengths to the beam-splitter, for the signal beam, respectively. L_0 is the pathlength for the idler beam.

around the $\delta x = 0$ position because, in this case, no two photons experience the same pathlength. The result of the experiment, shown in Fig. 4, however, does show an interference dip at this central position and it has high visibility.

To explain this phenomenon it helps to examine all potential pathways of the two photons as clearly shown in Feynman-like diagrams with space along one axis and time along the other [15]. Several interesting features become evident. First, it is clear in Fig. 5 that there are four possible path amplitudes in the description of the biphoton probability. Second, photon pairs are not detected at the same time. Third, the photons do not overlap in time at the beam-splitter, negating the possibility of a local-interaction picture explaining any result. Two of the paths have D1 firing Δt *before* D2, and the other two have D1 firing Δt *after* D2; these two types of firings are distinguishable in principle, but in this experiment Δt is not resolved by the discrimination window of the coincidence counter. In this treatment, despite the lack of experimental resolution, all the amplitudes distinguishable in *principle* are taken into account. Hence, all

four paths, which are indistinguishable *in this experiment*, are nonetheless summed and squared. This analysis by SPS is different from that of HOM because here the biphoton state is expanded according to its

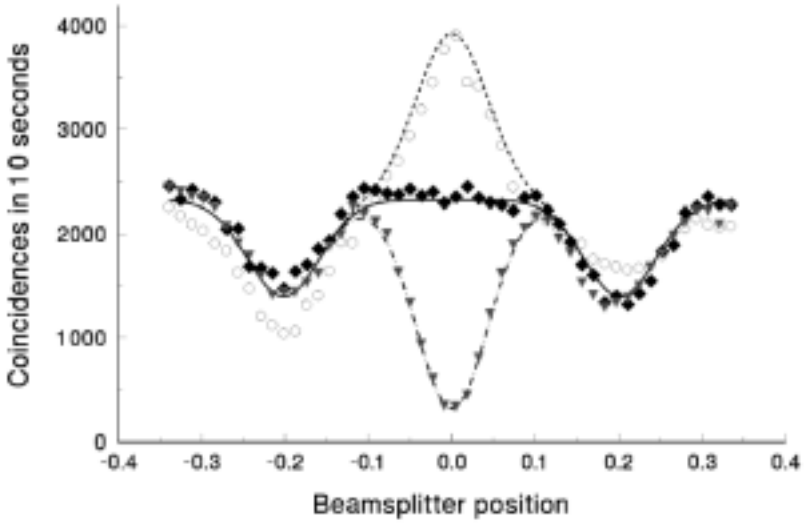

Fig. 4. Experimental results of the SPS experiment with the high-contrast center peak (after Strekalov, *et al.*, 1998) [15].

possible path amplitudes and is treated as interfering with itself, rather than the more classical concept of photons fields interfering with each other.

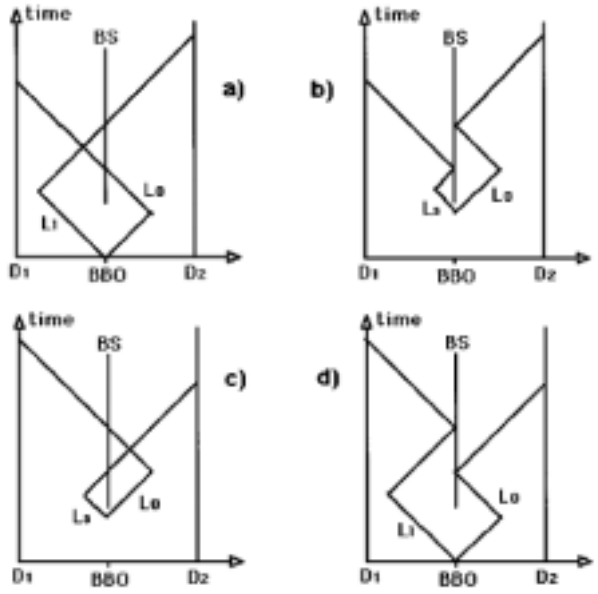

Fig.5. Feynman-like diagrams showing the different path possibilities of the biphoton state (after Strekalov, *et al.*, 1998) [15].

To begin an explanation of the results, we follow the treatment of SPS throughout and start with the general equation for the rate of coincidence counts time-averaged over the detection time of detectors D1 and D2

$$R_c(x,\phi) \propto \frac{1}{T}\int_0^T\int_0^T dT_1 dT_2 \left\langle \Psi \left| \hat{E}_1^- \hat{E}_2^- \hat{E}_1^+ \hat{E}_2^+ \right| \Psi \right\rangle \tag{12}$$

where T is the integration time associated with the coincidence counter, $T_{1,2}$ are the absolute detection times such that $T_1 - T_2$ is the amount of time between counts of the detectors. With $|\Psi\rangle$ defined as Eq. (5), we get

$$\left\langle \Psi \left| \hat{E}_1^- \hat{E}_2^- \hat{E}_1^+ \hat{E}_2^+ \right| \Psi \right\rangle = \left| \left\langle 0 \left| \hat{E}_1^+ \hat{E}_2^+ \right| \Psi \right\rangle \right|^2 \equiv \left| \Psi(T_1, T_2) \right|^2 \tag{13}$$

where $\Psi(T_1, T_2)$ is the biphoton state in terms of the absolute detection times. To put this in more meaningful notation let $t_j = T_j - (L_j / c)$ where L_j is the pathlength taken to the *j*th detector and let

$$T_- = T_1 - T_2 \quad T_+ = T_1 + T_2 \quad t_- = t_1 - t_2 \quad t_+ = t_1 + t_2 \quad T_{L,S} = (L_{L,S} + L_0)/c. \tag{14}$$

Rearranging, we get two expressions discriminating the four amplitudes easily. The first,

$$t_- = T_- \pm \Delta t, \tag{15}$$

discriminates amplitude set {(a),(b)} from set {(c),(d)} (referring to cases in Fig. 5), or, which ones had D1 fire before D2 vs. the other way around. The second,

$$t_+ = T_+ - T_{L,S}, \tag{16}$$

discriminates amplitude set {(a),(d)} from set {(b),(c)}, or, which set had a photon going along L_L vs. L_S. Hence, it is apparent that the four amplitudes can be completely distinguished in a basis recognizing 1) which detector fires first and 2) which path, L_S or L_L, was taken by the signal beam. Having established notation completely determining all amplitudes, we may finally express,

$$\Psi(t_-, t_+) = A(T_- - \tau, T_+ - T_L) + A(T_- - \tau, T_+ - T_S) + A(T_- + \tau, T_+ - T_S) + A(T_- + \tau, T_+ - T_L) \tag{17}$$

where reference [3] shows each amplitude term can be written in the form

$$A(t_-, t_+) = A_0 e^{-\sigma_+^2 t_+^2} e^{-\sigma_-^2 t_-^2} e^{-i\pi c t_+ / \lambda_p} . \tag{18}$$

In Eq. (18), σ_+ is the coherence time of the pump laser and can be considered constant over the detection time, T; $\sigma_- = c/2l_{coh}$ is associated with the coherence time of the biphoton itself, which is not resolved in the longer detection time, T. In this way, the Gaussian envelope functions in Eq. (18) have the effect of keeping all the different amplitudes indistinguishable in this setup. Substituting Eq. (18) into the following reconfigured equation equivalent to Eq. (12),

$$R_c(x,\phi) \propto \frac{1}{T} \int_0^T \int_0^T dT_- dT_+ \left|\Psi(t_-, t_+)\right|^2 , \tag{19}$$

to get

$$R_c = 1 - \cos\phi \exp\left(-x^2/l_{coh}^2\right) - \frac{1}{2}\exp\left\{-\left(-\frac{x-\Delta L/2}{l_{coh}}\right)^2\right\} - \frac{1}{2}\exp\left\{-\left(-\frac{x+\Delta L/2}{l_{coh}}\right)^2\right\}.$$

We can now explain all of Fig. 4. These three terms agree with the experiment remarkably well and are present in Fig. 4 as lines following the data. The central peak is modulated by $\cos\phi$ where ϕ is the nominal phase difference between beams exiting the L_L vs. L_S pathlengths. This phase was controlled to determine the sense of the peak. It is interesting to note that the central interference pattern arises for a setting of the beam-splitter which, classically, would not allow interference.

IV. CONCLUSION

Two experiments have been examined. The HOM experiment introduces the idea of mixing SPDC-produced entangled photons on a beam-splitter and interference effects are explained by the signal and idler photons' quantized electric fields undergoing fourth-order interference. However, the HOM method does not generally predict the outcome of the biphoton experiment. The SPS experiment intends to demonstrate the necessity of considering the single biphoton state as the entangled signal and idler photons. Only by describing the biphoton state in terms of all distinguishable path probability amplitudes are the SPS results understood. This approach considers the signal and idler photons as entangled sub-systems of the biphoton state. Hence, it is not generally correct to treat the interference of entangled photon states as individual photon wave packets interfering with each other -- despite the fact that quantum optical experiments of this type have traditionally been referred to as two-photon interferometry.

[1] M. O. Scully and M. S. Zubairy, *Quantum Optics* (Cambridge University Press, Cambridge, 1997)

[2] W.H. Louisell, A. Yariv, and A. E. Siegman, Phys. Rev. **124**, 1646 (1961)

[3] M. H. Rubin, D. N. Klyshko, Y. H. Shih, and A. V. Sergienko, Phys. Rev. A. **50**, 5122 (1994)

[4] R. J. Glauber, Phys. Rev. **130**, 2529 (1963); **131**, 2766 (1963)

[5] D. Bohm, *Quantum Theory* (Dover Publications, New York, 1951)

[6] T. J. Herzog, P. G. Kwiat, H. Weinfurter, A. Zeilinger, Phys. Rev. Lett. **75**, 3034 (1995)

[7] D. V. Strekalov, Y. -H. Kim, Y. Shih, Phys. Rev. A. **60**, 2685 (1999)

[8] R. Ghosh, C. K. Hong, Z. Y. Ou, and L. Mandel, Phys. Rev. A. **34,** 3962 (1986)

[9] C. K. Hong, Z. Y. Ou, and L. Mandel, Phys. Rev. Lett. **59**, 2044 (1987)

[10] L. Mandel, Rev. Mod. Phys **71**, S274 (1999)

[11] J. D. Franson, Phys. Rev. Lett. **62**, 2205 (1989)

[12] J. G. Rarity, P. R. Tapster, E. Jakeman, T. Larchuk, R. A. Campos, M. C. Teich, and B. E. A. Saleh, Phys. Rev. Lett. **65**, 1349 (1990)

[13] T. B. Pittman, D. V. Strekalov, A. Migdall, M. H. Rubin, A. V. Sergienko, and Y. H. Shih, Phys Rev. Lett. **77**, 1917 (1996)

[14] P. G. Kwiat, W. A. Vareka, C. K. Hong, H. Nathel, R. Y. Chiao, Phys. Rev. A. **41,** 2910 (1990)

[15] D. V. Strekalov, T. B. Pittman, and Y. H. Shih, Phys. Rev. A. **57**, 567 (1998)